Molecular Contamination Studies
by Molecular Beam Scattering

H. Nuss, Industrieanlagen-Betriebsgesellschaft mbH (IABG)
D-8012 Ottobrunn/Munich

A B S T R A C T

The capability of molecular beam scattering from a solid
surface for identification of molecular contamination of
the surface was studied. The experimental approach using
a thermal molecular beam source, a phase sensitive measur-
ing technique and a vapor effusion source for defined
contaminant application are described. The scattering
distribution measured for a N_2 molecular beam interact-
ing with a Platinum surface were measured for clean and
those conditions contaminated by diffusion pump oil
DC 705. An expression for the equilibrium of adsorption
and desorption rate was derived. Comparing the measured
dependency of the molecular beam intensity from surface
temperature with the theoretically derived formula for
the surface coverage offers a method to determine the
desorption energy. The applied method allows to identify
a surface coverage of DC 705 oil of approximately $2 \cdot 10^{-2}$
monolayers.

1. Introduction

Optical and thermal control surfaces of spacecraft components and experiments have been shown to be sensitive to the effects of contaminant deposition. Ultraviolet radiation can cause chemical reactions that result in changes of reflectivity and absorptance/emittance characteristics of the surfaces. For the studies of degradation effects by various organic films the influences during prelaunch testing in space simulation chambers and the effects of contamination during missions have to be considered. Limitations on performance of infrared telescopes operated on a Space Shuttle Orbiter or on Spacelab are imposed by the contaminant atmosphere of the spacecraft. To keep fluctuations in background radiation below the noise equivalent power of the best detectors anticipated for the 1980s a limit on the column density of infrared active molecules of approximately 10^{12} molecules cm^{-2} was recommended [1].

The purpose of this paper is to report the capability of molecular beam interaction with a solid surface for detecting molecular contamination of a surface by an organic film.

The influence of contamination on the scattering distributions of molecular beams was reported in different papers [2] [3]. The theoretical description of the scattering distributions in the region of speculary directed scattering is in good agreement with the hard-cube-theory [4]. The aspect of molecular beam interaction with a solid surface for satellite applications was studied, too [5].

The measuring principle to be applied in this study is based on the change of the scattering distribution of a molecular beam from a clean surface and from a contaminated surface.

The adsorption and desorption rates caused by the residual gas (clean surface) and by the deposited contaminant DC 705 (contaminated surface) will be estimated. An adsorption isobar will be derived which defines the relationship between surface coverage and surface temperature. By comparing the temperature dependence of the scattered beam intensity and of the surface coverage the desorption energy can be determined.

2. Experimental Approach

A plan view of the experimental setup is shown in Fig. 1. The work chamber [6] in which the scattering experiments were conducted was evacuated by adsorption pumps and an ion pump of 400 l/s pumping speed. To the main vacuum chamber a vapor effusion source is attached for the deposition of molecular contamination films. The work chamber assembly was furnished with a molecular beam source, sample holder adapter and heater, and a molecular beam detector and phase sensitive measuring setup [7].

2.1 Molecular Beam Source

The production for molecular beams characterized by almost complete freedom from intermolecular collisions is possible by producing a certain vapor pressure in an

Sample holder of WCA

Sample holder adapter and Pt surface

Beam chopper, light and photocell

Collimating tube

Beam source tube

To needle valve and gas reservoir

Flange to diffusion pump

Molecular beam source port

Rotatable Ion gauge
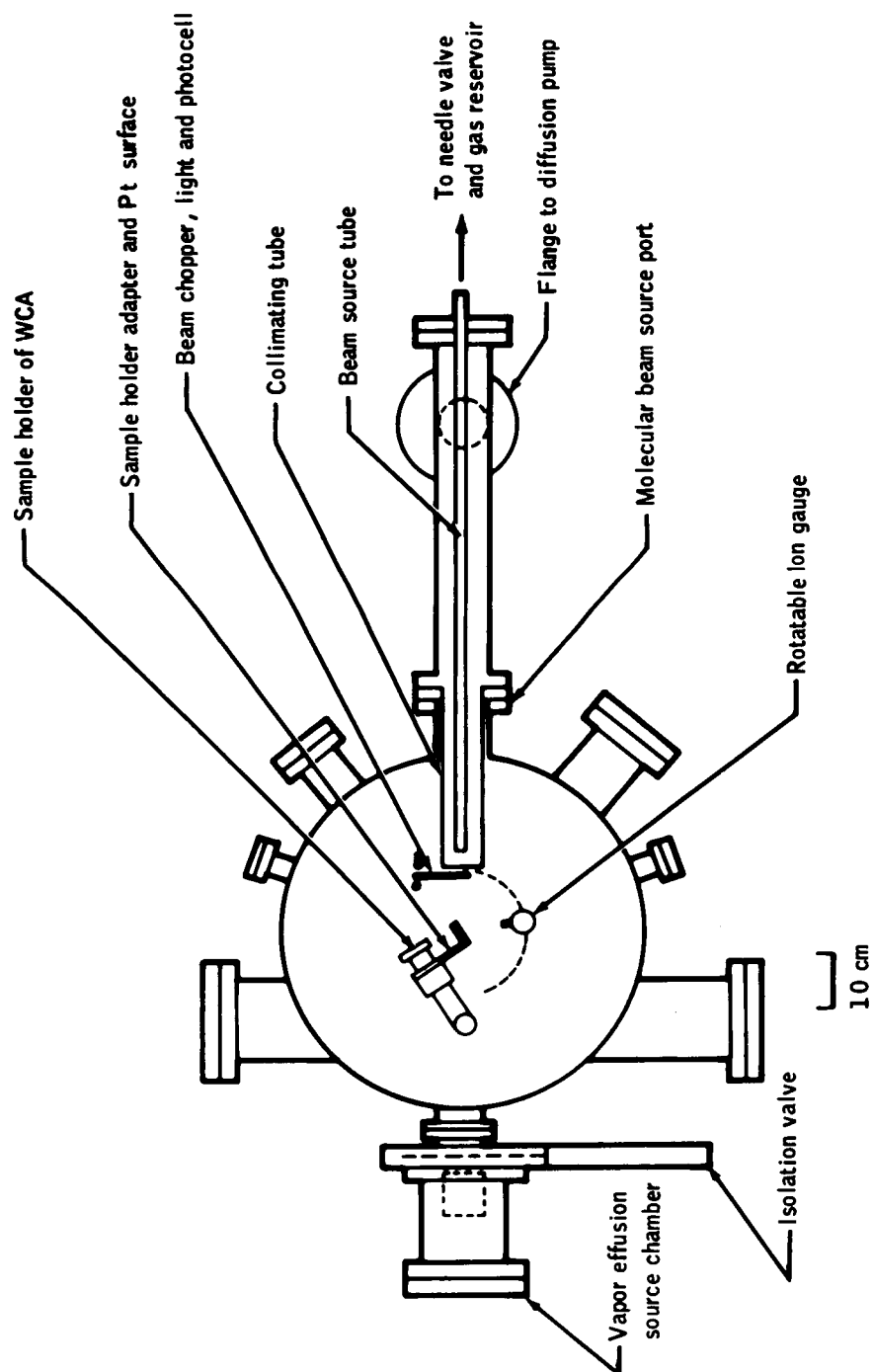
10 cm

Isolation valve

Vapor effusion source chamber

Fig. 1: Plan view of the experimental setup

enclosure with a well defined exit opening into a vacuum chamber.

For molecular flow conditions the total number N of particles per second escaping through an aperture of the enclosure is [8]

$$N = \frac{p_s A_s}{(2 \pi m k T_s)^{1/2}} = 3.51 \cdot 10^{22} \frac{p_s A_s}{(M T_s)^{1/2}} \qquad (1)$$

p_s : Pressure in enclosure, mbar

A_s : Area of ideal aperture, cm^2

T_s : Temperature in enclosure, K

m : Mass of particle, g

M : Molar mass of vapor, $g\ mole^{-1}$

k : Boltzmann constant, $mbar\ cm^3\ K^{-1}$

The number of particles per second striking a target of unit area on the axis of the aperture at a distance r from the aperture is:

$$I(o) = \frac{n_s v_a A_s}{4 \pi r^2} = 1.11 \cdot 10^{22} \frac{p_s A_s}{r^2 (M T_s)^{1/2}} \qquad (2)$$

n_s : number of particles per unit volume
in enclosure, molecules cm^{-3}

v_a : average molecular velocity, $cm\ s^{-1}$

Considering a cylindrical channel instead of an ideal
aperture, the cylindrical channel being of length l and
radius a the total number of particles per second given
by equation (1) is reduced by the Clausing factor to
N_1:

$$N_1 = \frac{8a}{3l} \frac{p_s A_s}{(2mkT_s)^{1/2}} \tag{3}$$

The optimum orifice geometry for the delivery of the
maximum fraction of effusing molecules onto a target is
a long cylindrical aperture [9]. This type of aperture
was used for the molecular beam source which consists
of the beam source tube and the collimating tube
(Fig. 2). An oil diffusion pump system with a liquid
nitrogen cooled cold trap and an optically dense water
cooled baffle served as the pumping system for the beam
source. The beam source tube was attached to a manifold
with a variable needle valve and gas reservoir.

2.2 Phase Sensitive Measuring Setup

According to the equations (1) to (3) it can be esti-
mated that for a pressure in the enclosure of $p_s = 10^{-1}$
mbar for a collimated beam of particles drawn from the

Beam source tube

Collimating tube

12mm

1mm

$r_{SC} = 12$mm

1mm

α_1: Angle of incidence

α_3: Scattering angle

Ion collector
of beam detector

$r_{EC} = 55$mm

$r_{PTD} = 60$mm

$r_{CPt} = 60$mm

α_3

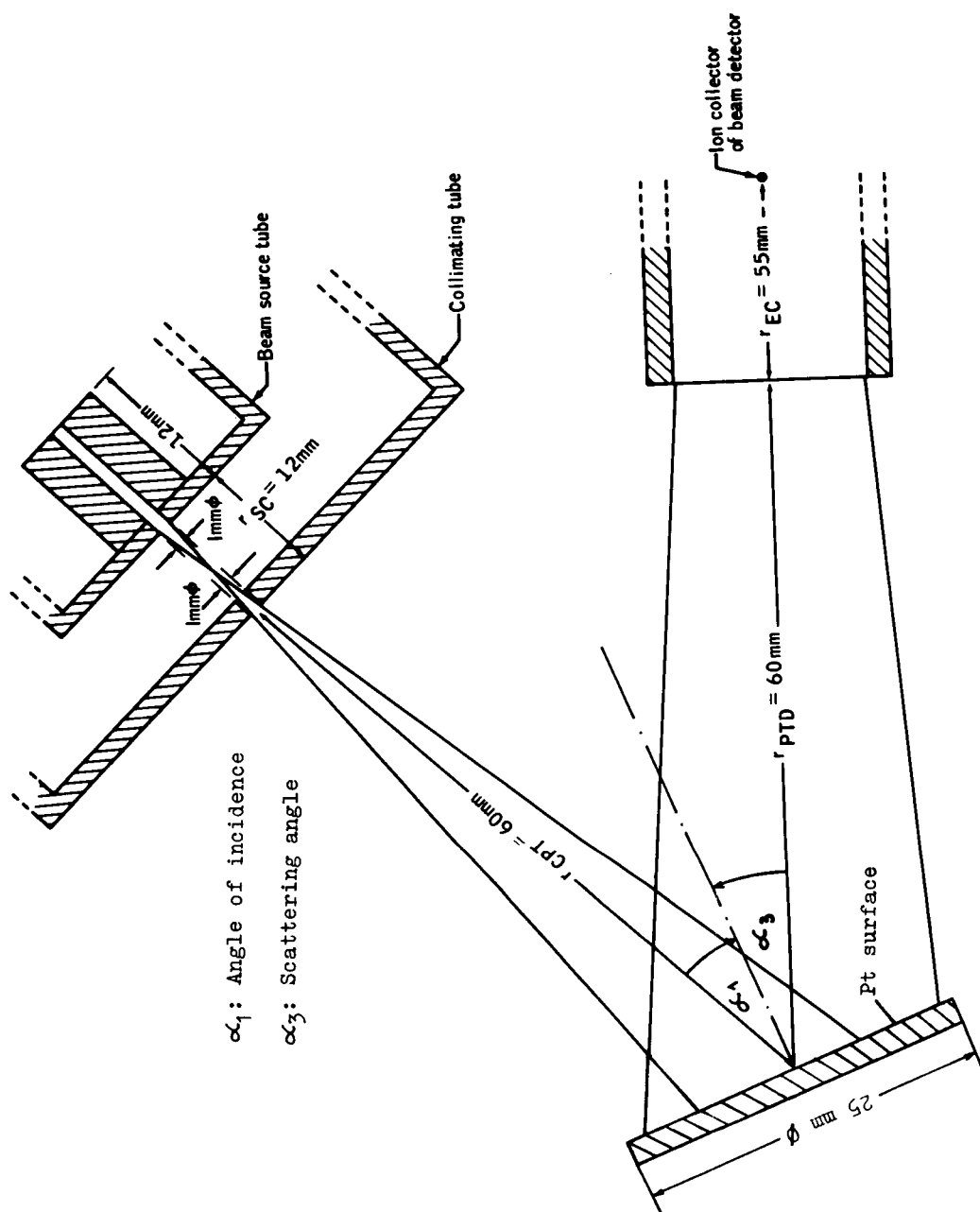α_4

Pt surface

25 mm ϕ

Fig. 2: Geometry of scattering experiment

molecular beam source and taken far enough away for an
experiment conveniently to be conducted, the density is
in the order of magnitude 10^9 particles/cm^3. This must
be compared to a density of particles in the residual
gas in the chamber, which is approximately $4 \cdot 10^{10}$
particles/cm^3 for a pressure of 10^{-6} mbar. Because of
the slow fluctuations and drifts in ordinary vacuum
systems for measuring a signal of 1 part in 40 an ac
method has to be applied [10]. The molecular beam was
modulated by a mechanical chopper and the desired
signal could be identified by its specific frequency
and phase using a phase lock-in amplifier. A differ-
entially pumped system was used for increasing the
signal-to-noise ratio.

2.3 Scattering Surface

The sample on which the scattering experiments were
carried out was a Platinum surface produced by sputter-
ing. The substrate was a quartz sample (25 mm ∅, 6 mm
thick). The thickness of the Platinum film was 1200 Å
± 200 Å. The crystallite size shown in the transmission
electron microscope was approximately 100 Å. The
diffraction patterns indicate that there was no texture
in the foil. A nichrome wire heated the sample by
radiation up to 400°C.

2.4 Vapor Effusion Source (Fig. 3)

The vapor effusion source [1] which is separated by an
isolation valve from the main chamber was used for the
deposition of high molecular weight organic contaminant
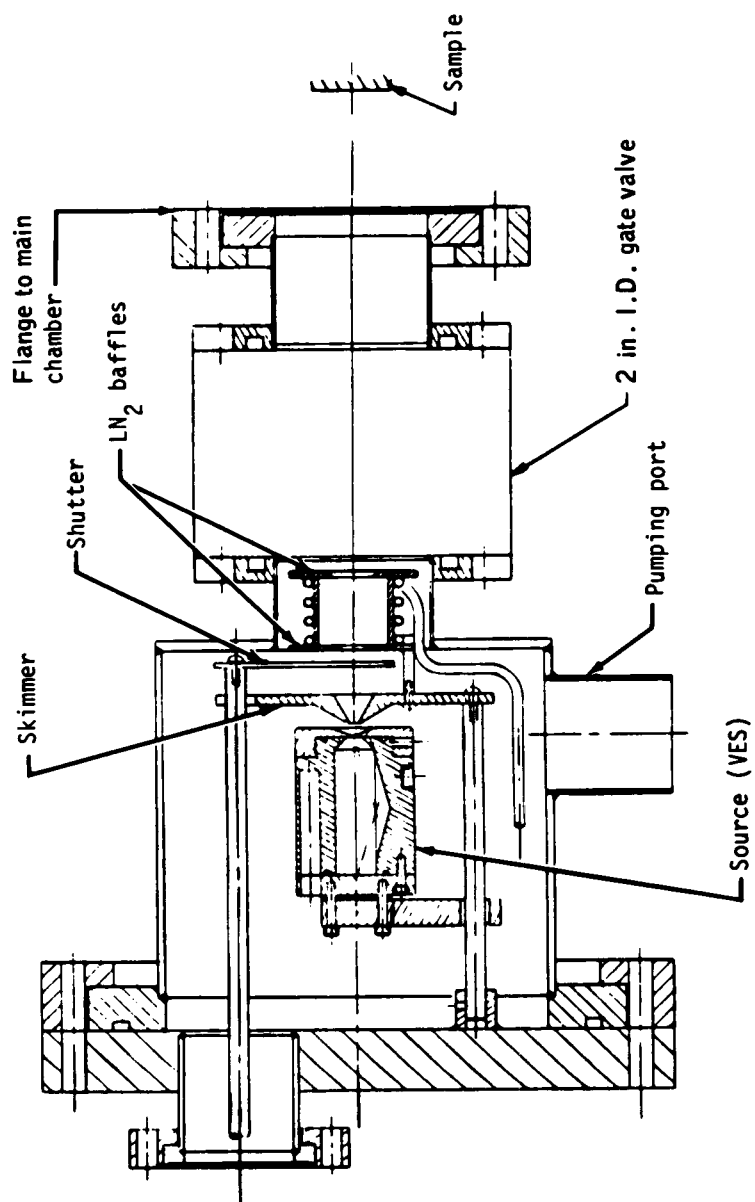films onto the surface. A combination of three apertures

Fig. 3: Vapor effusion source chamber

Sample

Flange to main chamber

LN₂ baffles

Shutter

Skimmer

2 in. I.D. gate valve

Pumping port

Source (VES)

(a beam skimmer and two liquid-nitrogen cooled colli-
mators) limit the cross section of the beam to the
diameter of the sample. For the measurements the source
was filled with DC 705 pentaphenyl trimethyl siloxane
diffusion pump oil. The vapor pressure in the source
can be changed by variation of the source temperature.

3. Experimental Results

3.1 Primary Molecular Beam (Fig. 4)

The angular distribution measurements of the primary
beam [7] were carried out to determine the intensity
dependence from the pressure in the beam source p_s,
for signal-to-noise ratio measurements, and for checking
the angular solution of the molecular beam detector. In
Fig. 4 the primary intensity of a He molecular beam as
a function of angle α_2 with respect to surface normal
of the beam source is plotted. The distribution shows
the directivity of the source caused by the long
cylindrical channels used as beam source and collimating
apertures.

3.2 Scattering Distribution

In Fig. 5 the normalized scattered intensity I/I_o
(I_o refers to the intensity for $\alpha_3 = 0$) as a function
of scattering angle α_3 is shown. In the temperature
range 39 to 129°C the measured scattering distribution
is "approximately diffuse"; for a surface temperature
of 210°C a specularly directed distribution is found.
A reversible transition between diffuse and specularly
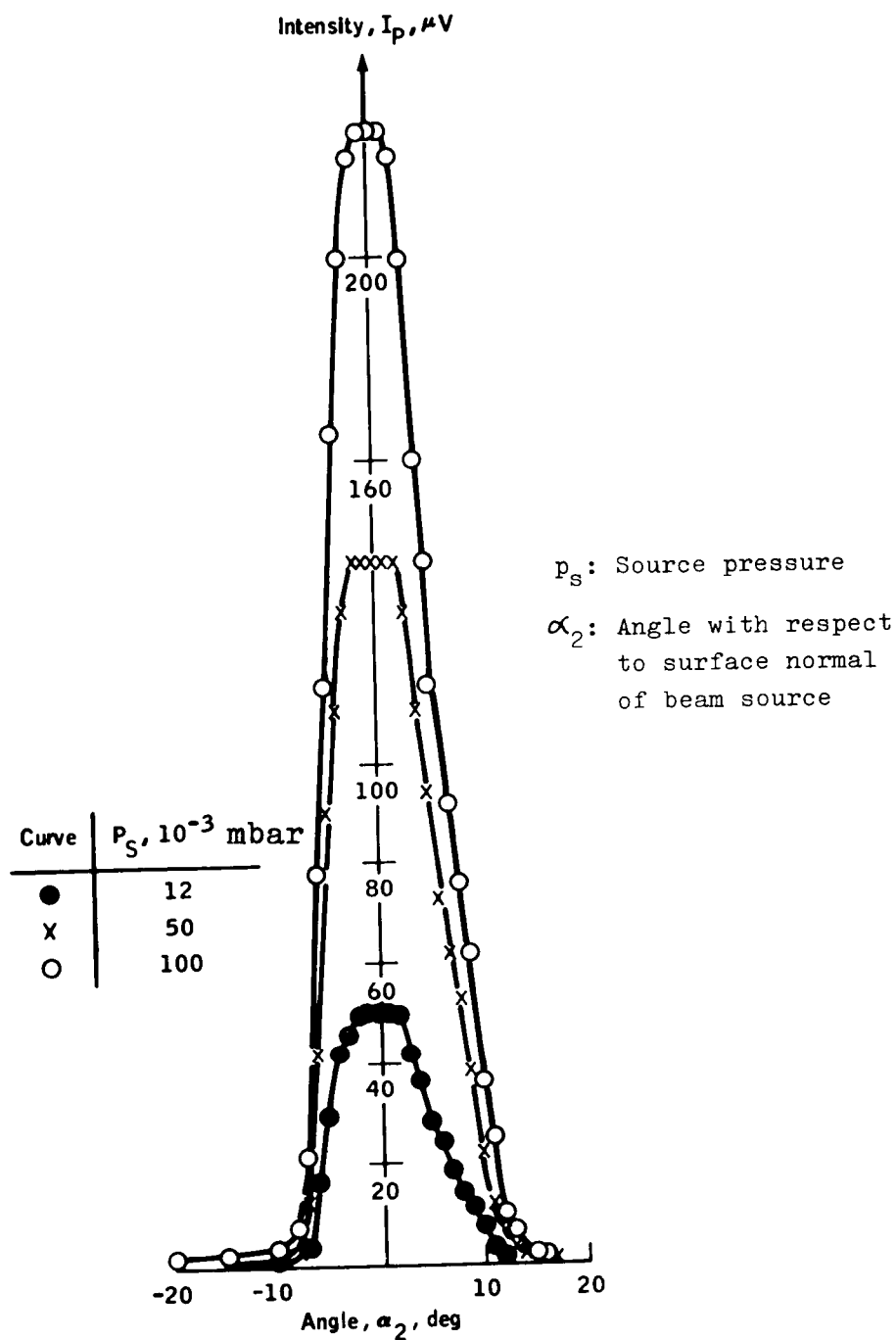directed scattering at a surface temperature of about
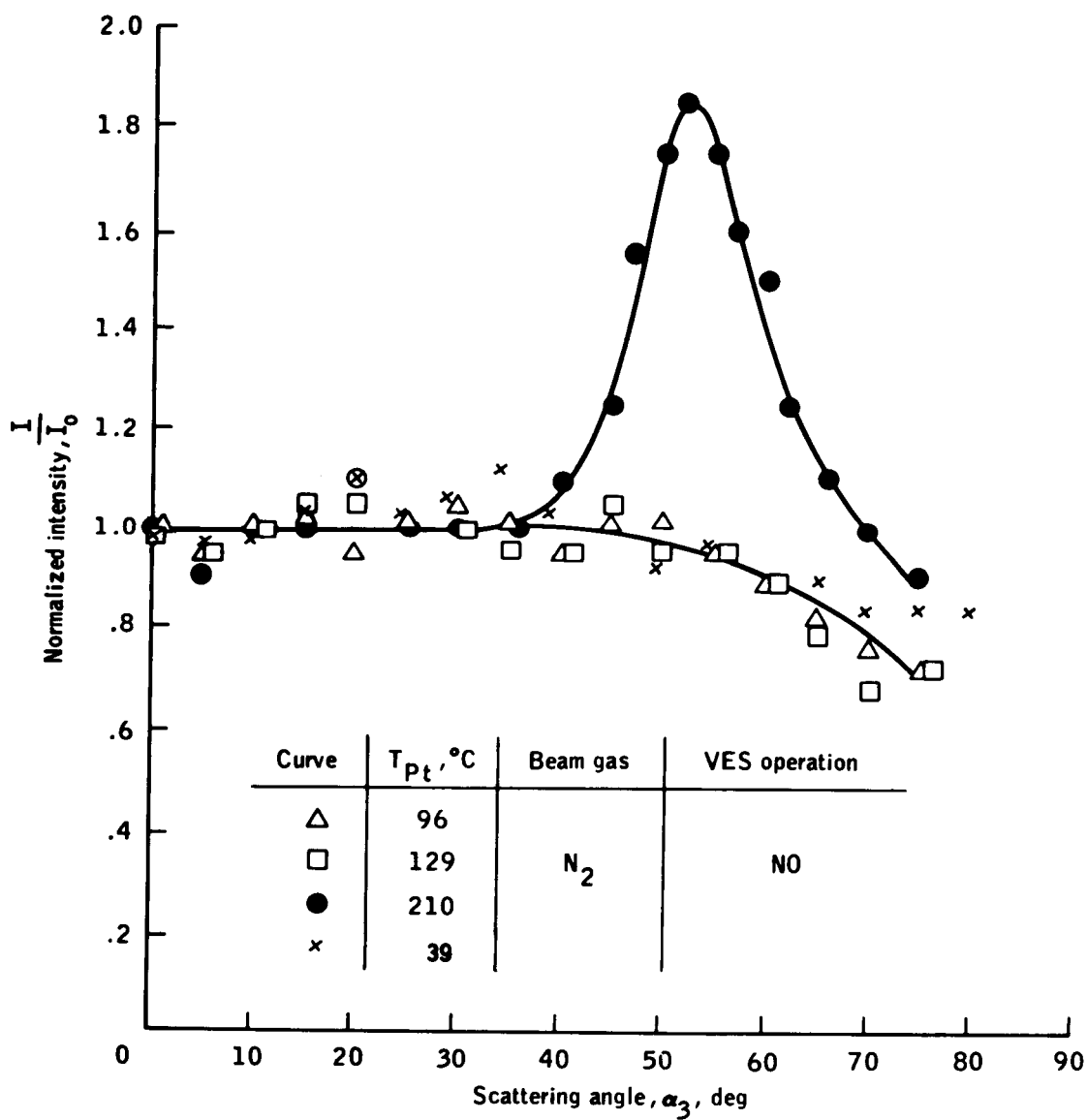
Fig. 4: Primary molecular beam intensity

Fig. 5: Scattering distribution for surface
temperatures 39 to 210 $^{\circ}$C
angle of incidence $\alpha_1 = 62^{\circ}$

$200^{\circ}C$ is explained by removal of adsorbed residual gas layers [2] [3].

For an angle of incidence of $\alpha_1 = 62^{\circ}$ the maximum specularly directed beam intensity is measured for a scattering angle of $\alpha_3 = 52^{\circ}$ (subspecular scattering [3]). In Fig. 6 the maximum scattered beam intensity as a function of surface temperature is plotted. The intensity starts to increase at a temperature of approximately $160^{\circ}C$ and increases in the entire measured temperature range up to $210^{\circ}C$.

3.3 Scattering Distribution for Contaminated Surface

In Fig. 7 the intensity distribution of the scattered molecular beam is displayed after the vapor effusion source was operated with a vapor pressure of $p_s = 5 \cdot 10^{-9}$ mbar. No specularly directed beam could be measured for surface temperatures up to $213^{\circ}C$. For a surface temperature of $360^{\circ}C$ similar results as indicated in Fig. 5 were found: A specularly directed beam with a width and a maximum scattered beam intensity comparable to the values measured for the clean surface for a surface temperature of $210^{\circ}C$.

In Fig. 8 the normalized intensity I/I_0 for an incidence angle $\alpha_1 = 55^{\circ}$ and a scattering angle $\alpha_3 = 45^{\circ}$ is plotted as a function of surface temperature. The increase of the scattered beam intensity starts after the contamination at a surface temperature of $220^{\circ}C$. The necessary temperature to reach a value of 1.5 for the ratio of the scattered beam intensity for high surface
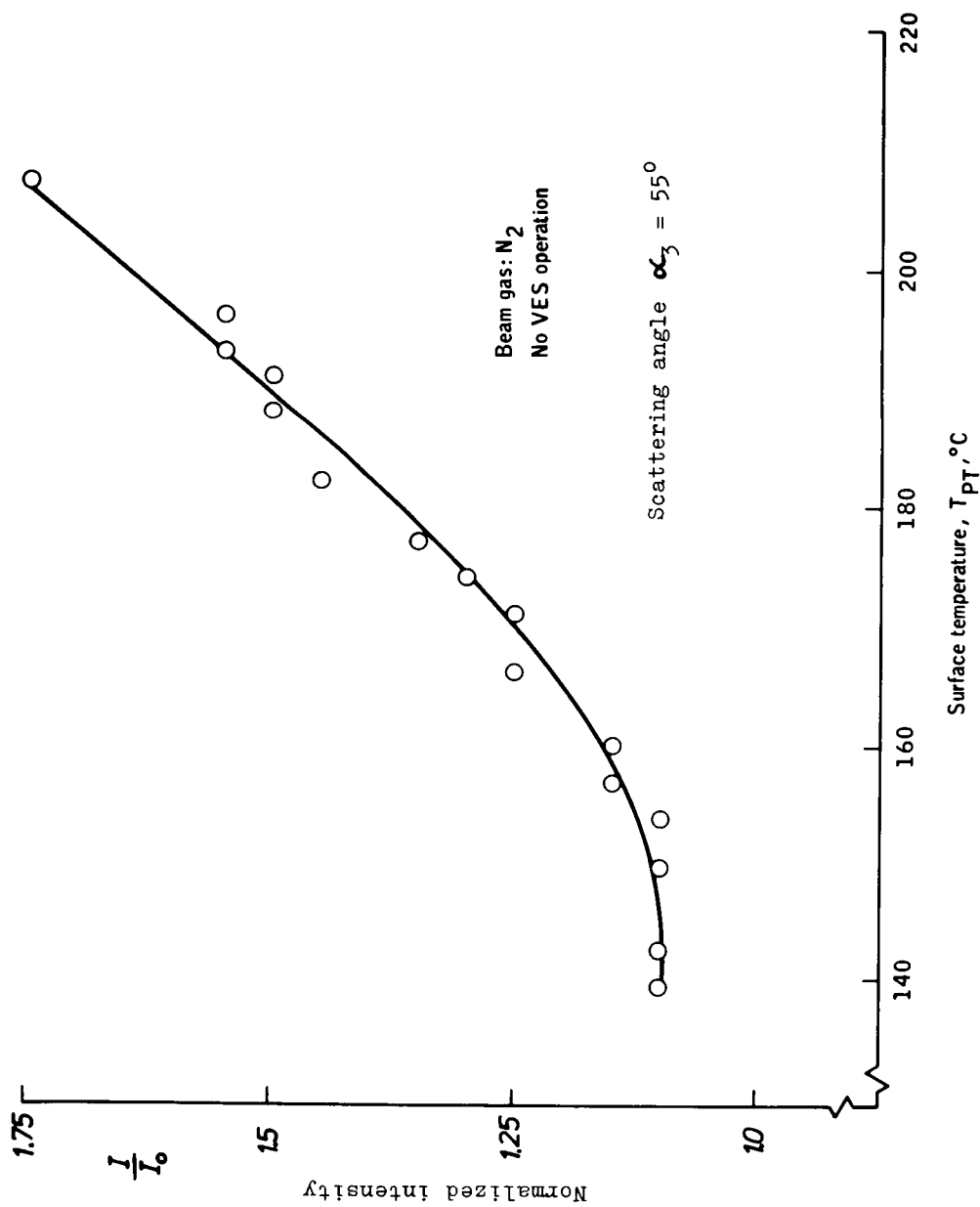
669

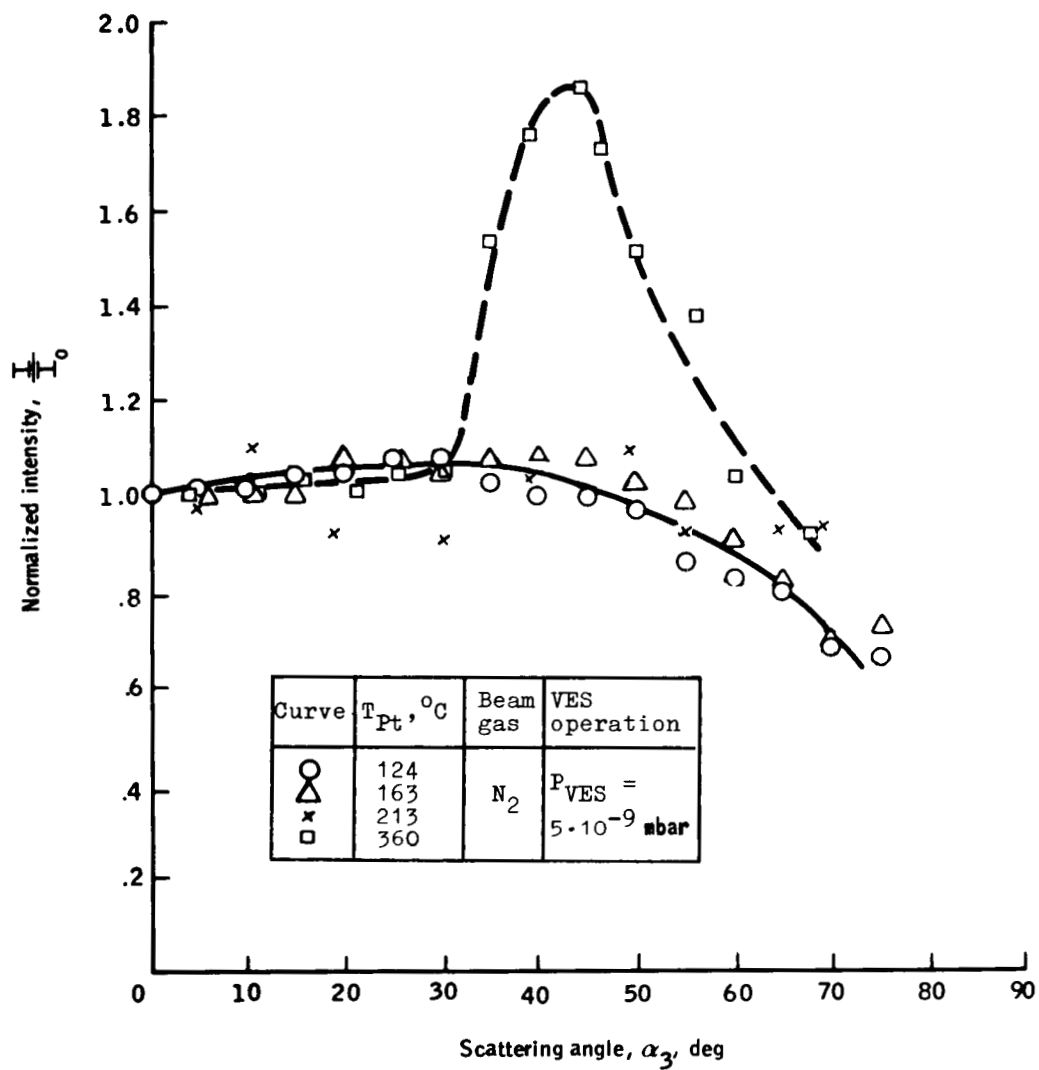Fig. 6: Scattered beam intensity as a function of surface temperature

Normalized intensity, $\frac{I}{I_o}$

Scattering angle, α_3, deg

Curve	T_{Pt}, $^\circ$C	Beam gas	VES operation
○ △ ✗ □	124 163 213 360	N_2	$P_{VES} =$ $5 \cdot 10^{-9}$ mbar

Fig. 7: Scattering distribution for surface temperatures 124 $^\circ$C to 360 $^\circ$C after operation of vapor effusion source (VES), angle of incidence $\alpha_1 = 55^\circ$
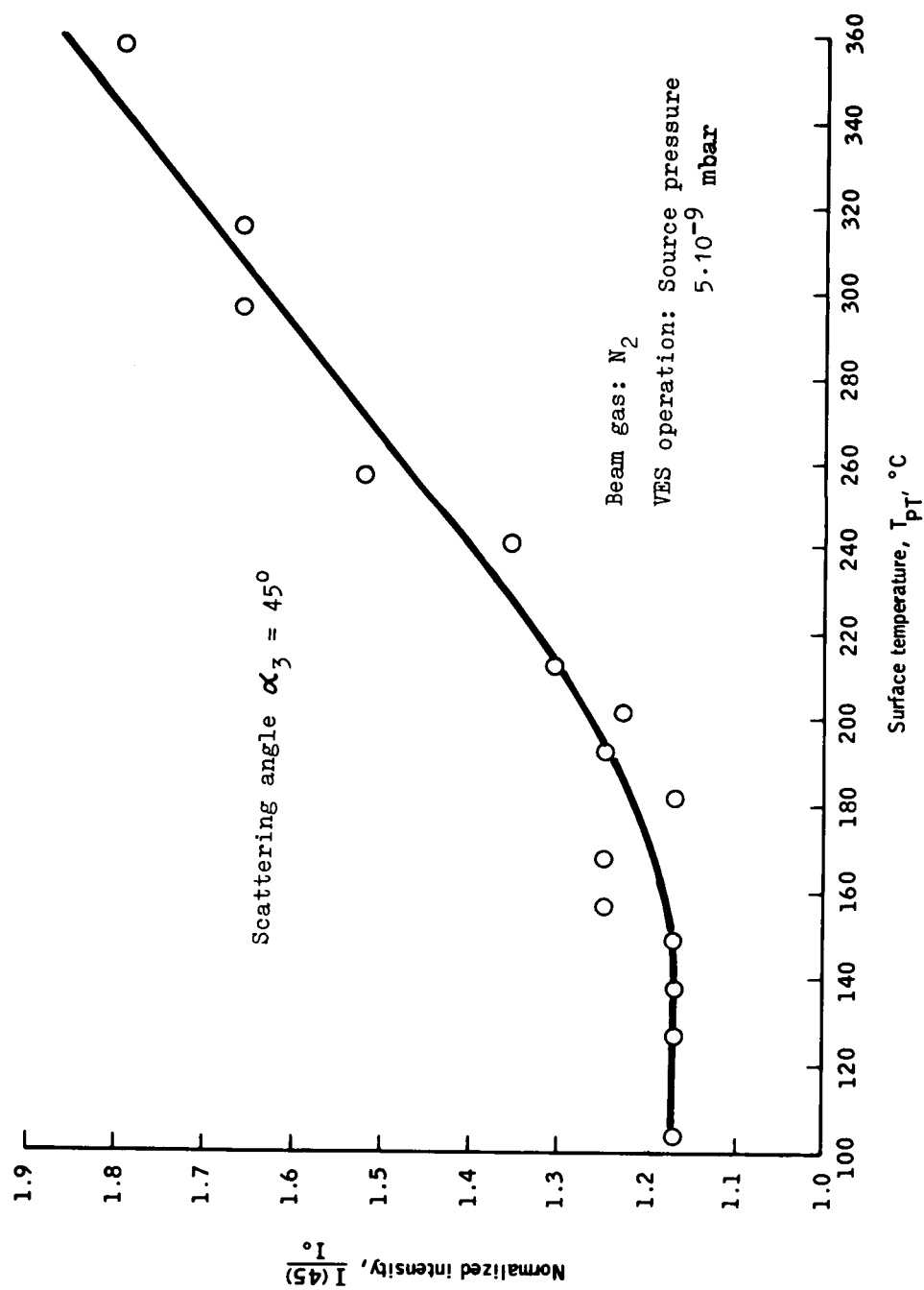
Fig. 8: Scattered beam intensity as a function of surface temperature after operation of vapor effusion source (VES)

temperature and low temperature was 210 $^\circ$C before contamination and 360 $^\circ$ C after contamination.

4. Interpretation and Discussion of the Experimental Results

The objective of this paragraph is the theoretical explanation of the different experimental results described in paragraph 3.2 and 3.3 for a clean and a contaminated surface. In the following the adsorption and desorption rates caused by the residual gas (clean surface) and by the deposited contaminant DC 705 (contaminated surface) will be estimated.

The scattered molecular beam intensity was measured as a function of surface temperature. For the determination of the scattered intensity dependence from surface coverage an adsorption isobar will be derived which defines the relationship between surface coverage and surface temperature.

The rate of desorption from unit surface area may be written as [11]:

$$- \frac{d\sigma}{dt} = \frac{\sigma}{\tau_0} \exp(- \frac{E_A}{RT}) \tag{4}$$

σ : Number of adsorbed molecules per cm^2 for not dissociating molecules, molecules cm^{-2}

τ_o : Time of oscillation of the molecules in the adsorbed state, seconds

E_A : Energy of adsorption, cal mole^{-1}

R : Molar gas constant, cal mole K^{-1}

The adsorption rate is [12)]

$$\frac{d\sigma}{dt} = \alpha\, N_A\, f(\frac{\sigma}{\sigma_o}) \tag{5}$$

α : Probability for adsorption of a molecule hitting an uncovered surface area

N_A : Number of molecules per second and cm^2 arriving on the surface, molecules $cm^{-2}s^{-1}$

σ_o : Number of adsorbed molecules for a monomolecular layer, molecules cm^{-2}

With the assumption of Langmuir that every molecule, which strikes a molecule already adsorbed, returns to the gas phase, the following expression is valid [13)]:

$$f(\frac{\sigma}{\sigma_o}) = 1 - \frac{\sigma}{\sigma_o} \tag{6}$$

Denoting $\theta = \frac{\sigma}{\sigma_o}$ as the degree of covering from
equations (4), (5) and (6) for equilibrium conditions
can be written:

$$\theta = \cfrac{1}{1 + \cfrac{\sigma_0}{\tau_0 \propto N_A} \, \exp(- \frac{E_A}{RT})} \qquad (7)$$

According to kinetic gas theory the number of molecules
per second and cm^2 N_A arriving on a surface for a
particle density n and average velocity v_a is:

$$N_A = \frac{nv_a}{4} \qquad (8)$$

With equation (8) the expression for the degree of
covering according to equation (7) is as follows:

$$\theta = \cfrac{1}{1 + \cfrac{4\,\sigma_0}{\tau_0 \propto nv_a} \, \exp(- \frac{E_A}{RT})} \qquad (9)$$

To get a relationship between the degree of covering θ and the scattered beam intensity showing a specularly directed portion (Fig. 5, 6 and 7, 8) the curves of Fig. 6 and 8 were approximated by linear functions. In the temperature range, in which the scattered beam intensity increases with temperature (Fig. 6, 8) a linear decrease of the degree of covering θ is assumed. With this procedure the degree of covering θ can be calculated from the data of Fig. 6 and 8. Plotting θ determined by the measured beam intensity in the form $\ln (\frac{1}{\theta} - 1)$ as a function of $\frac{1}{T}$ gives the adsorption energy E_A as the slope in this plot (according to equation (9)). This method is an approximation neglecting the dependence of E_A from temperature and degree of covering in the temperature range covered by the experiments. Evaluating the value for the adsorption energy E_A for the surface temperature range in which the scattered beam intensity $\frac{I}{T}$ is proportional to the surface temperature (Fig.6) results in a value of $E_A = 23$ kcal/mole for surface conditions without operating the vapor effusion source. This value corresponds approximately to the value for desorbing water vapor considering the tightly bound last monolayer [14]. Having determined the approximate value for the adsorption energy E_A by this method the degree of covering θ can be calculated from equation (9).

In Fig. 9 the calculated degree of covering θ_{Res} due to residual gases as a function of surface temperature is displayed for different values of adsorption energy E_A and of particle density n. Taking the mean values for
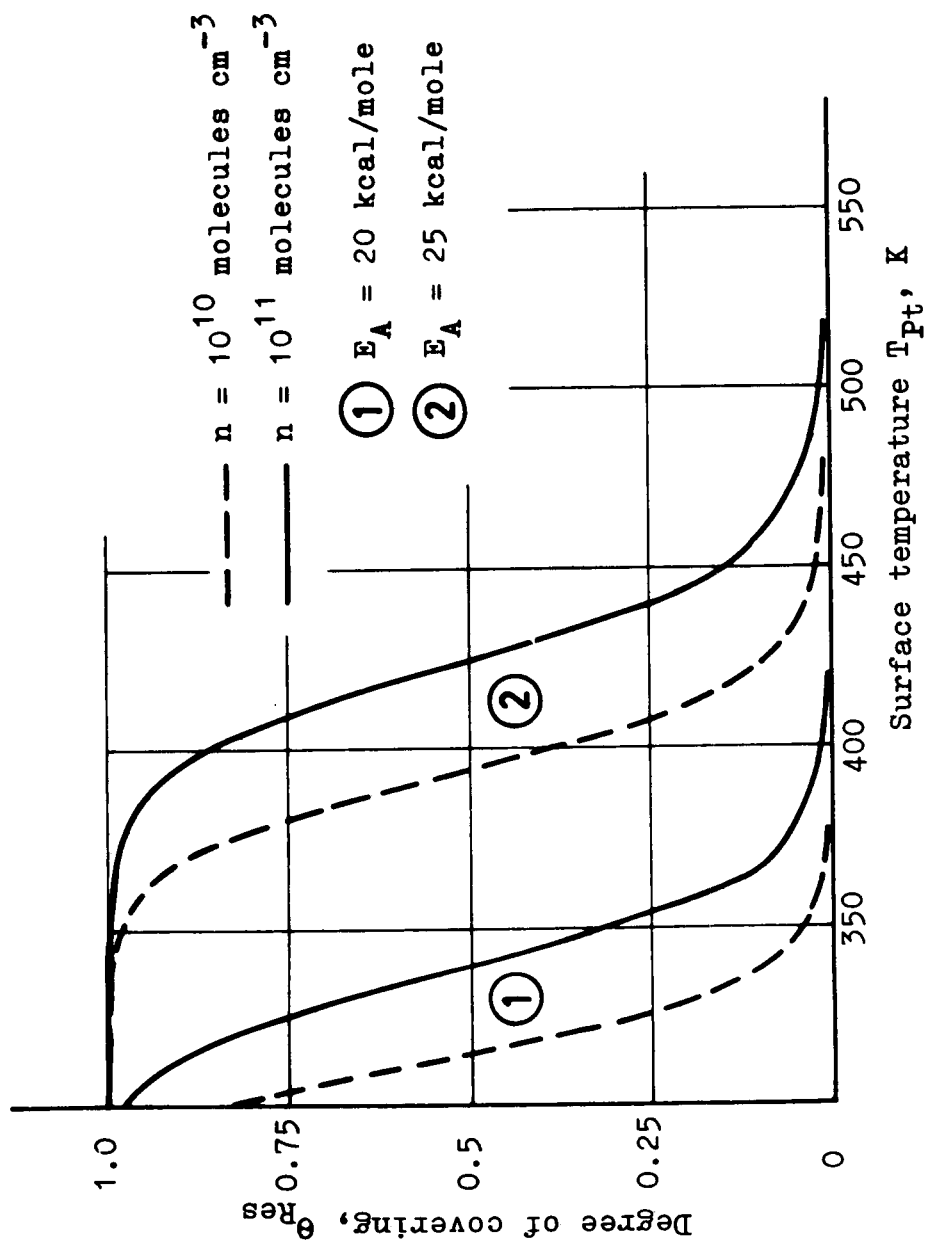
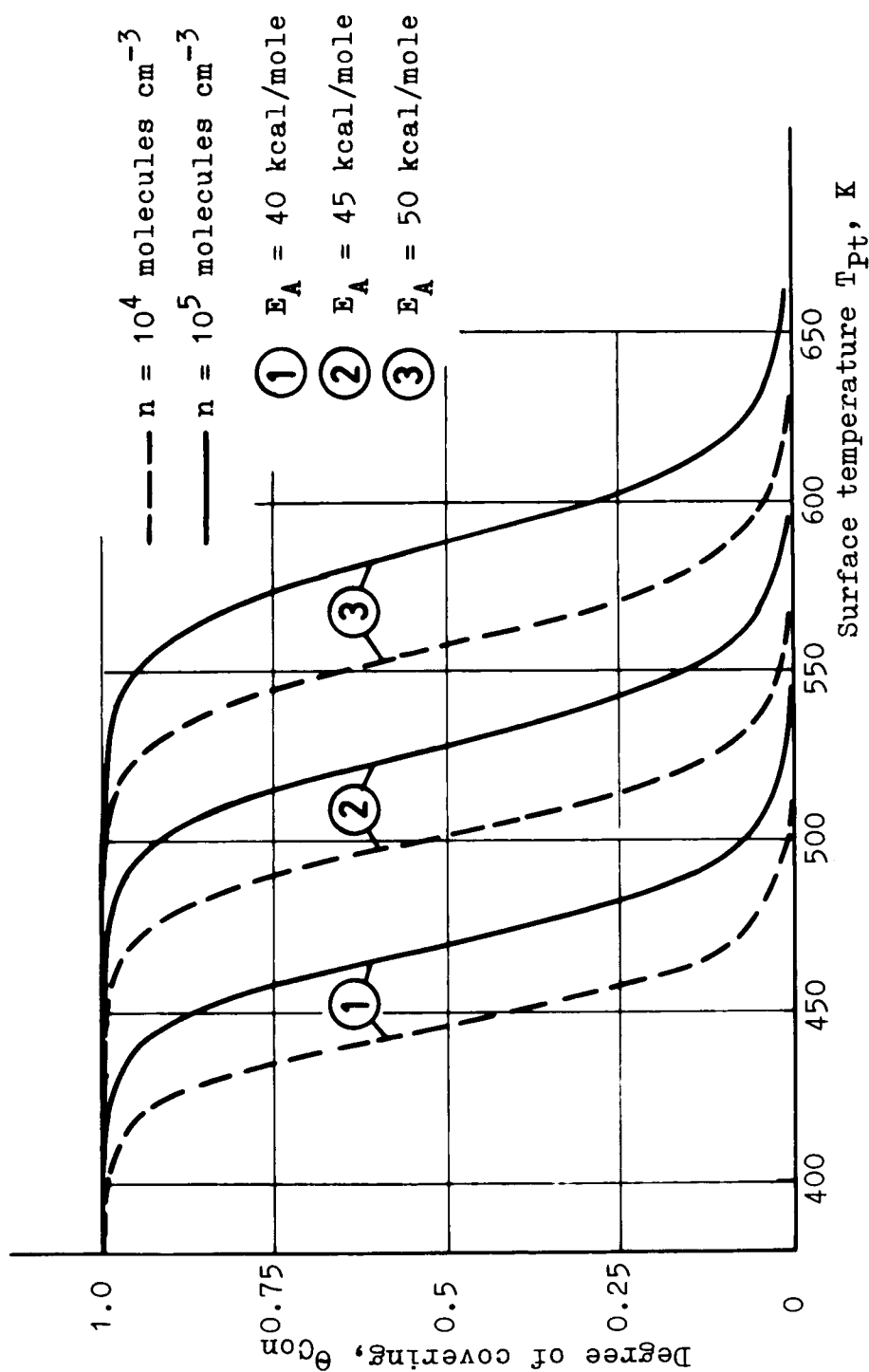Fig. 9: Calculated degree of covering Θ_{Res} due to residual gases as function of surface temperature

Fig. 10: Calculated degree of covering θ_{Cont} due to contaminant deposition as function of surface temperature

the experimental conditions of $\sigma_o = 10^{15}$ molecules cm^{-2} and $n = 10^{11}$ molecules cm^{-3} results in a covering degree $\theta_{Res} = 3 \cdot 10^{-2}$ monolayers (for a surface temperature of $210^\circ C$ and an adsorption energy of 25 kcal/mole) which can be identified by measuring a scattering distribution with a specularly directed beam as shown in Fig. 5.

By application of the above mentioned method for the contaminated surface an adsorption energy for DC 705 can be evaluated of 52 kcal/mole. In Fig. 10 the calculated degree of covering θ_{Con} due to contaminant deposition as a function of surface temperature is displayed for different values of adsorption energy E_A and of particle density n. The latter was estimated with the aid of the formula of paragraph 2. For the experimental conditions of $\sigma_o = 10^{14}$ molecules cm^{-2} and $n = 10^4$ molecules cm^{-3} a covering degree $\theta_{Con} = 2 \cdot 10^{-2}$ monolayers can be calculated (for a surface temperature of $360^\circ C$ and an adsorption energy of 52 kcal/mole) which can be identified by measuring a scattering distribution with a specularly directed beam as shown in Fig. 7.

The results indicate that molecular beam scattering from solid surfaces is capable to identify contamination of a surface by some hundredth of monolayers.

5. Acknowledgement

6. References

1. Simpson, J.P.; Witteborn, F.C; Effect of the Shuttle Contaminant Environment on a Sensitive Infrared Telescope, Applied Optics, Vol. 16, 1977, p. 2051

2. West, L.A.; Kozak, E.I.; Somorjai, G.A., Molecular Beam Scattering from Single Crystal Surfaces under Ultrahigh Vacuum Conditions, J. Vacuum Sci. Technol. 8, 1971, p. 430-436

3. Smith, J.N.; Saltsburg, H.: Atomic-Beam Scattering from Epitaxially Grown Gold Films, J. Chem. Physc. 40, 1964, p. 3585

4. Logan, R.M.; Stickney, R.E., Simple Classical Model for the Scattering of Gas Atoms from a Solid Surface, J. Chem. Phys. 44, 1966, p. 195-201

5. Evlanov, E.N.; Lebedev, Yu.V.; Leonas, V.B.: On the Possible Method of Gas- Satellite Surface Interaction Studies, Proc. 9th Intern. Symp. Rarefied Gas Dynamics, 1974 DFVLR Press, Porz-Wahn, West-Germany, 1974, p. E 16-1

6. Dillow, C.F.; Allen, T.H.; Linford, R.M.F.; Richmond R.G., A System for the Study of Molecular Contamination, NASA SP 379, 1975, p. 623

7. Nuss, H.E., Molecular Contamination Study by Interaction of a Molecular Beam with a Platinum Surface, NASA TMX-58169, 1976

8. Hughes, V.W.: Schulz, H.L. (Editors): Atomic and Electron Physics Part A, Atomic Sources and Detectors, Academic Press, New York, 1967, pp. 155-198 and 390-414

9. Freeman, R.D.: Molecular Flow and the Effusion Process in the Measurement of Vapor Pressures, Report ASD-TDR-63-754, Pt III, 1967

10. Brackmann, R.T.; Fite, W.L.: Condensation of Atomic and Molecular Hydrogen at Low Temperatures, J. Chem. Phys. 34, 1964, p. 1572

11. Redhead, P.A., Thermal Desorption of Gases, Vacuum 12, p. 203-211

12. D. Jaeger: Einfluss von an der Oberflaeche adsorbier-ten Gasteilchen und Einfluss von Struktur auf die Gas-Festkoerper-Wechselwirkung gemessen an der Molekular-strahlstreuung, Deutsche Luft- und Raumfahrt, Forschungsbericht 73-14

13. de Boer, J.H.: The Dynamical Character of Adsorption, Clarendon Press, Oxford, 1968, p. 54

14. Griffith, J.S.: Some Tests for the Increase in Friction of Mechanisms of the Mariner Mars 1969 Spacecraft in the JPL Molsink Space Simulation Chamber, AIAA/ASTM/IES 4th Space Simulation Conf. 1969, Paper 69-996